Chapter 2
Information Extraction Techniques in Chemical Sensing

Thiago Matheus Guimarães Selva, Tiago Luiz Ferreira and Thiago Regis Longo Cesar Paixão

In order to produce an analytically useful signal, as mentioned in the previous chapter, we need to transduce chemical information using an instrumental technique. Numerous analytical chemistry techniques exist for the extraction of chemical information, e.g. spectrometry, separation techniques coupled with spectroscopic detection, or electrochemical and other methods. However, mainly due to the cost and necessity of portability, electrochemical and colorimetric techniques are frequently used to translate chemical information into a readable output for the analysts and users in in-field applications of chemical sensors. This chapter will introduce the concepts involved in these techniques, which are mainly used to extract information for fabricating chemical sensors.

2.1 Electrochemical Sensors

Essentially, the electrochemical sensors are classified as: conductimetric, potentiometric, and amperometric or voltammetric sensors.

T.M.G. Selva
Instituto Federal de Educação, Ciência e Tecnologia de Pernambuco,
Avenida Prof. Luiz Freire, 500, 50740-540 Recife, PE, Brazil

T.M.G. Selva · T.R.L.C. Paixão (✉)
Departamento de Química Fundamental, Instituto de Química,
Universidade de São Paulo, Avenida Prof. Lineu Prestes, 748,
05508-000 São Paulo, SP, Brazil
e-mail: trlcp@iq.usp.br

T.L. Ferreira (✉)
Instituto de Ciências Ambientais, Químicas e Farmacêuticas,
Universidade Federal de São Paulo, Rua Prof. Artur Riedel, 275,
09972-270 Diadema, SP, Brazil
e-mail: tlferreira@unifesp.br

T.R.L.C. Paixão and S.M. Reddy (eds.), *Materials for Chemical Sensing*,
DOI 10.1007/978-3-319-47835-7_2

2.1.1 Conductimetric Sensors

Conductimetric sensors are based on measuring the ionic conductance of solutions. This conductance results from the individual contributions of each ion in the solution; it is therefore a property that does not depend on the specific reaction levels of an electrode, as opposed to, for example, voltammetric sensors.

Conductimetric sensors can be employed in direct conductometry, where electrolyte concentration is determined by a single conductance measurement, or relative conductometry, where conductance is monitored during titration, and the end point is determined from the collected data.

Since these sensors measure electrical conductance arising from all ionic species present in solution, they do not respond to specific ions. This specificity may be achieved by a separation technique, such as chromatography or capillary electrophoresis, employing conductimetric sensors for the detection of charged species of interest.

The conductance of a solution or a solid material can be expressed by Ohm′s law, Eq. 2.1:

$$I = G \times E \tag{2.1}$$

where I is the electric current flowing through a solution or a solid, E is the potential difference, and G is the conductance. Generally, Ohm′s law is expressed in terms of resistance, Eq. 2.2:

$$E = R \times I \tag{2.2}$$

which leads to the definition of G as the inverse of resistance, Eq. 2.3:

$$G = \frac{1}{R} \tag{2.3}$$

The resistance or conductance of a specimen depends on its temperature, chemical nature, homogeneity, size, and shape. For solutions, the conductance also depends on the number of ions present.

For a specimen uniform over its whole length:

$$G = \kappa \times \frac{A}{l} \tag{2.4}$$

where A is the cross-sectional area of the specimen, and l is its length. The proportionality constant κ is called conductivity (Fig. 2.1). The same relation is valid for a solution between two electrodes (Fig. 2.1).

Experimentally, either the resistance or the conductance of a solution is measured to determine κ. The basic experimentally measured parameter in both cases is the solution resistance, but modern conductance bridges are calibrated to directly

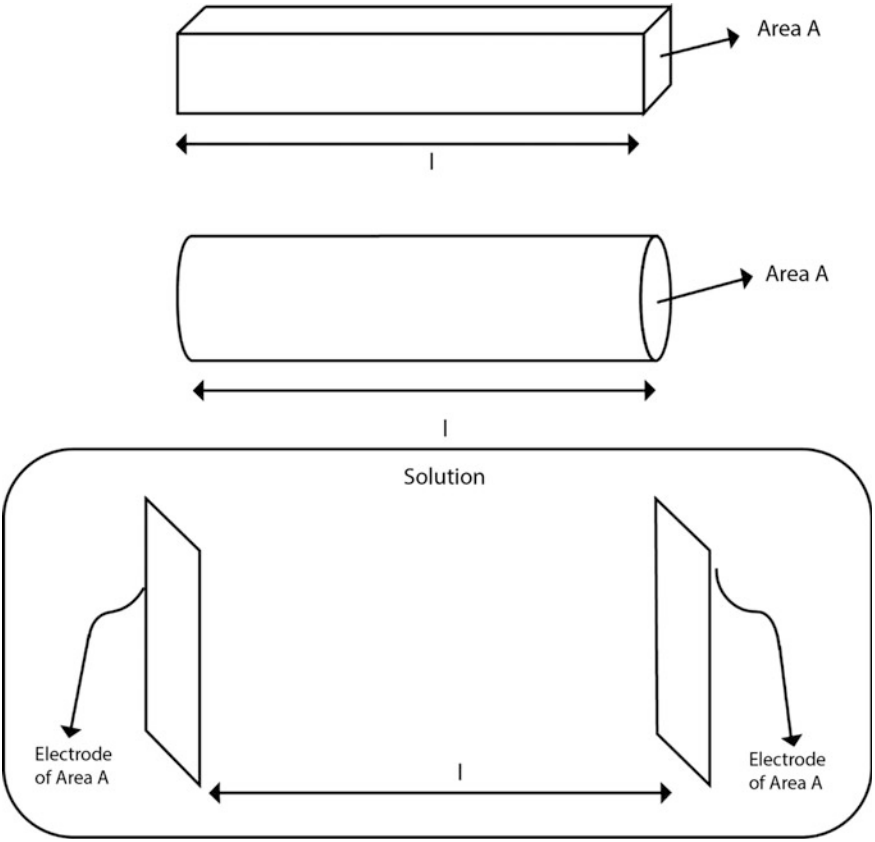

Fig. 2.1 Schematic representation of solid and electrolytic conductors

provide conductance read-outs. The experimental set-up is based on a Wheatstone bridge apparatus.

When studying the conductivity of a solution, it is essential that the concentration remains constant throughout the measurement. Passage of an electric current through a solution induces chemical reactions at the electrodes, resulting in changes in the solution concentration. These reactions or their effects must be avoided in conductivity measurements. This is achieved by changing the direction of the current, so that the reactions are continually reversed and have no net chemical effect. Alternating current is generally used, e.g. one having a frequency of 1000 Hz.

The current passing through a solution is created by the movement of ions contained therein. The amount of ions present is likely to be inversely proportional to the resistance of the solution and directly proportional to its conductivity, κ. Experiments show that κ varies considerably with concentration.

Further discussion and procedures can be found in textbooks on conductimetric titrations, determination of dissociation constants of weak electrolytes, etc. [1, 2].

This notwithstanding, there are two important cases of interesting applications of conductimetric sensors: (i) measurement of solution conductance employing electrodes outside the solution (oscillometry) and (ii) measurement of conductance of an array of modified sensors as an electronic nose.

Oscillometry is often employed for conductance measurements in corrosive solutions, e.g. ones that could damage the cell electrodes. In order to measure the conductance of a solution using this procedure, the electrodes are positioned outside the solution, on the external wall of the conductance cell. To perform these measurements, equipment capable of operating at high frequencies is required (ca. 10^6 Hz). An interesting application of oscillometry is the use of contactless conductimetric cells in capillary electrophoresis to detect different charged species as they are separated by electroosmotic flow. In these cases, the conductimetric cell is positioned on an appropriate portion of the external wall of the capillary [3].

The second case deals with smell identification using an array of interdigitated electrodes modified with a conducting polymer, where each electrode is modified with a different polymer. When gaseous molecules are absorbed by the polymer, its electrical conductivity is affected. Different gases affect the conductivity in different ways. These signal variations can provide a “digital impression” or “chemical fingerprint” of the studied vapour [4]. The electronic nose (E-nose) must be “trained” to recognize different smells through electrical conductivity using chemometric approaches described in Chap. 9.

2.1.2 Potentiometric Sensors

Potentiometric sensors work by measuring the equilibrium potential (potential of zero current) of the sensor versus a reference electrode. These potentials are a function of the activity of the species in solution. The equality of activity and concentration is reasonable to assume only for dilute solutions [5].

Typical instrumentation for potentiometric measurements includes a reference electrode and an indicator electrode (potentiometric sensor) connected to a high output impedance voltmeter (10^{12} Ω) [6].

There are two classes of potentiometric sensors: (i) metallic electrodes, i.e. electrodes that develop a potential determined by redox equilibria (Nernst equation) at the electrode–solution interface (e.g. platinum electrode) and (ii) ion-selective electrodes, where the difference of potentials across a membrane is measured, which is influenced by the activity of the species on either side of the membrane.

The use of metallic electrodes commonly brings poor selectivity if more than one redox couple is present in solution, since all couples contribute to the overall equilibrium potential. On the other hand, the potential generated for ion-selective electrodes (ISEs) is due to a selective interaction between the electrode membrane and an ion.

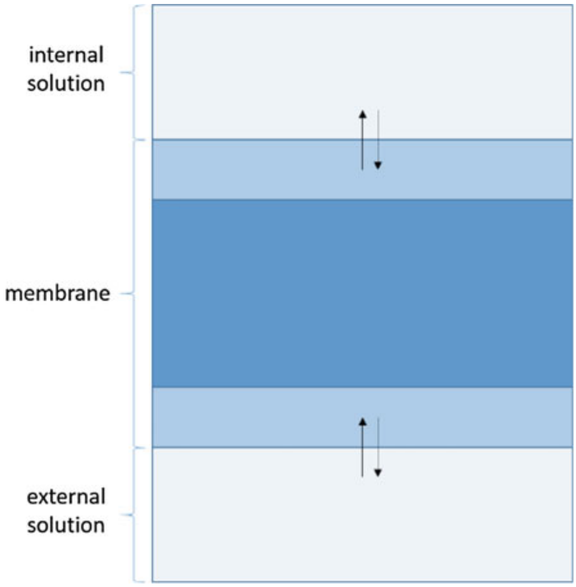

Fig. 2.2 Schematic representation of a membrane electrode. *Arrows* symbolize the exchange of ions across the membrane between the internal and external solutions

ISEs measure the potential difference created by the movement of ions between an internal and an external solution phase, delimited by the membrane (Fig. 2.2). The membrane potential, E_{membrane}, is given by Eq. 2.5:

$$E_{\mathrm{membrane}} = \frac{RT}{z_i F} \ln \frac{a_2}{a_1} \tag{2.5}$$

where R is the universal gas constant, T is the temperature in Kelvin, F is the Faraday constant, and a is the activity of an ion i of charge z_i. As the activity of the ion i in the internal solution is constant:

$$E_{\mathrm{membrane}} = c + \frac{RT}{z_i F} \ln a_2 \tag{2.6}$$

where c is a constant.

The membrane potential is measured by calculating the potential difference between an internal reference electrode and an external reference electrode. Thus, the membrane serves as a link between two halves of a concentration cell.

A perfect ISE responds to only one ion in a solution containing "any" ions. This ideal situation cannot be achieved, particularly when ions with similar properties are present in solution. The interference effects of other ions depend on their potentiometric selectivity coefficients, K_{ij}, according to the Nicolsky–Eisenman Eq. 2.7:

$$E_{\text{membrane}} = c + \frac{RT}{z_i F} \ln\left(a_2 + \sum K_{ij} \times a^{\frac{z_i}{z_j}}\right) \tag{2.7}$$

where j is the interfering species with charge z_j.

These selectivity coefficients can be evaluated by a fixed interference method (varying the primary ion activity at a constant level of interferent) or a separated method (comparing the response of the electrode in primary ion solution with that in a solution containing only the interferent ion with the same activity) [5].

Selective electrodes are divided into three classes:

(i) primary ion-selective electrodes;
(ii) compound or multiple-membrane ion-selective electrodes;
(iii) all-solid-state ion-selective electrodes.

2.1.2.1 Glass Electrodes

Glass electrodes were the first ISEs to be developed and are used mainly to measure pH. Glass is an amorphous solid consisting predominantly of silicates and is permeable to H^+, Na^+, and K^+. The composition of glass determines the permeability to each type of ion, but some interference always occurs.

The glass membrane must be conductive to serve as a potentiometric sensor. Conduction within the hydrated gel layer involves the movement of H^+. Sodium ions are the charge carriers in the dry interior of the membrane. This sensor functions by exchange of solution protons with sodium ions in the surface region, to a depth of ca. 50 nm.

$$H^+_{\text{solvent}} + Na^+_{\text{glass}} \rightleftarrows H^+_{\text{glass}} + Na^+_{\text{solvent}} \tag{2.8}$$

So, for low proton and high sodium concentrations in solution, this exchange is not complete and the observed potential is higher (pH is lower) than expected, according to Eq. 2.9 (Eisenman equation) for the interference of Na^+.

In strongly acidic or alkaline solutions, the activity coefficients of H^+ and Na^+

$$E_{\text{membrane}} = c + 0.0592 \log\left(a_{H^+} + \sum K_{\frac{Na^+}{H^+}} \times a_{Na^+}\right) \tag{2.9}$$

can significantly depend on the environment, possibly leading to a deviating potential. These deviations at high activities occur in all ISEs.

In pH measurement, the potential difference between two reference electrodes on both sides of the glass membrane is monitored. The two electrodes are often combined with the glass membrane (Fig. 2.3).

It is very important to calibrate the glass electrode prior to measurements due to the differences between its inner and outer surfaces, which lead to differences in the monitored potential. This potential contribution (often called asymmetry potential)

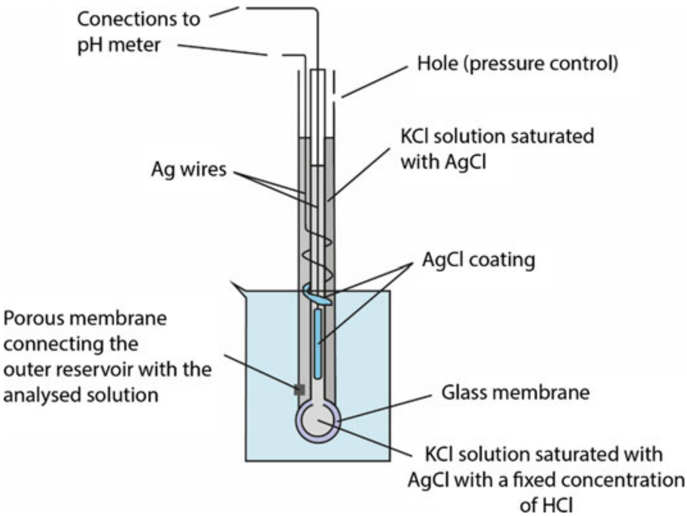

Fig. 2.3 Combined glass electrode for pH sensing

can also change with time when the electrode is used, making periodic calibration necessary [1, 6, 7].

2.1.2.2 Crystalline Membrane Electrodes

These potentiometric sensors are based on a solid-state crystalline membrane. The homogeneous membrane is an ionic solid with a low solubility product, and the sensed ion corresponds to the cationic or anionic constituent of the above membrane. The potential is created by ion exchange between the solution and the surface of the ionic crystal. Migration of crystal structure defects accounts for the charge transport through the membrane.

As these sensors respond to both the cation and anion of the solid membrane, it is expected that they would also be the main interfering species. The electrode is also sensitive to ions that can bind the membrane components, especially if the binding products have lower solubility than the membrane material.

Other crystalline membranes, called heterogeneous membranes, are based on an inert plastic matrix (e.g. PVC, silicone rubber, or conducting epoxy resin) with incorporated small crystals of the ionic solid.

Generally, this kind of potentiometric sensor does not use an internal reference electrode, but an ohmic contact [1].

2.1.2.3 Non-crystalline Membrane Electrodes

Non-crystalline membrane electrodes are based on a polymer-supported membrane containing solvent and an ion exchanger or neutral carrier (commonly a chelating agent) selective for the species to be determined. Transport across the membrane is achieved by exchange of the species of interest between adjacent chelating agents [1].

2.1.2.4 Gas-Sensing Electrodes

These potentiometric sensors are simple ISEs with a second gas-permeable membrane, which allows certain molecules to pass. Usually, a small amount of electrolyte solution is placed between the selective membrane and the outer membrane. The selective membrane is commonly a pH glass membrane, and the variation of pH is related to the partial pressure of the gas [1].

2.1.2.5 Potentiometric Enzyme Electrodes

These sensors also have a second membrane, which contains an immobilized enzyme. Since enzymes are highly specific catalysts, one of the products of an enzymatic reaction can be monitored and the analyte indirectly determined [1].

2.1.2.6 Ion-Selective Field-Effect Transistors

In order to miniaturize potentiometric sensors achieving reproducible signals with a high signal/noise ratio, ion-selective field-effect transistors (ISFETs) [8] were developed using semiconductor transistor technology (Fig. 2.4). The function of a conventional field-effect transistor is to respond to tiny voltage differences of a metallic gate between the source and drain, converting them into a low-impedance output signal (current signal).

In ISFETs, the metallic gate is replaced by an ion-selective membrane, which is in contact with solution. The drain signal (output) is directly related to the activity of ions in solution [8].

2.1.3 Voltammetric Sensors

Voltammetric sensors are based on measuring the relationship between the current and the applied potential. There are two main approaches to carry out voltammetric experiments: (i) measure the current response as a function of applied potential and (ii) monitor the potential response as a function of applied current. Most

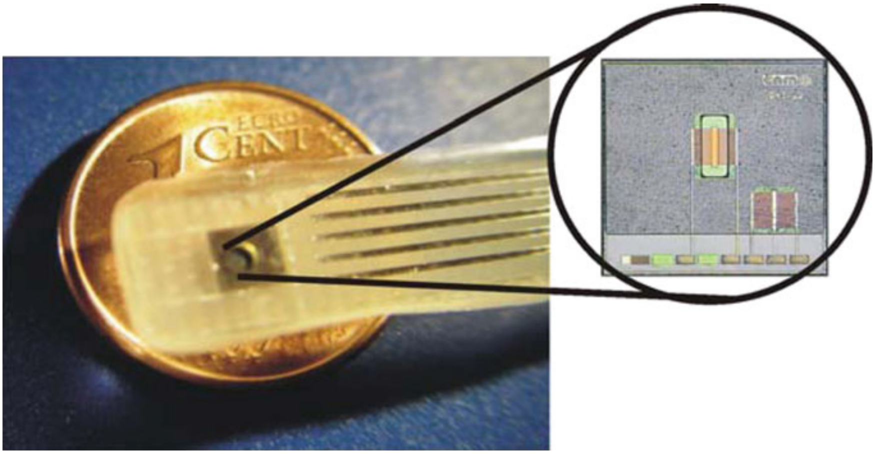

Fig. 2.4 ISFET for pH sensing. Reprinted from Jimenez-Jorquera et al. [8]. Copyright (2010), with the permission from MDPI®

voltammetric sensors are based on potential control. Amperometric sensors are a special kind of voltammetric sensors, where determination of electroactive species is performed at constant potential [5, 6, 9, 10].

The instrumentation for voltammetric sensors is more complex than that for conductimetric and potentiometric sensors. Three electrodes are necessary to avoid current passage through the reference electrode, which would change its potential. The current passes through an electrical circuit between the working electrode and an auxiliary electrode, with the reference electrode used to control the potential of the working electrode. A potentiostat is necessary to control the applied potential and register the current at the working electrode. To gain information on current-controlled experiments and monitor changes in the potential of the working electrode, a galvanostat is required.

The current of analytical interest in voltammetry is the faradaic current, which is generated by oxidation or reduction of the analyte at the surface of the working electrode. Another current, called a capacitive current, interferes with each measurement. For example, when the potentiostat forces the electron transfer for a reduction process to occur on the working electrode, bringing the potential to more negative (or less positive) values, the cations in the solution are attracted to the electrode surface, whereas anions are repelled. This flux of ions and electrons, i.e. the capacitive current, is not a contribution from the redox reaction and must be minimized in order to achieve lower voltammetric detection limits.

In voltammetry, the potential excitation signal can be imposed on a working electrode in different waveforms, with each potential waveform eliciting a characteristic current response (Fig. 2.5).

A classical voltammetry excitation signal is a linear potential scan, where the DC potential applied to the electrochemical cell varies linearly as a function of time.

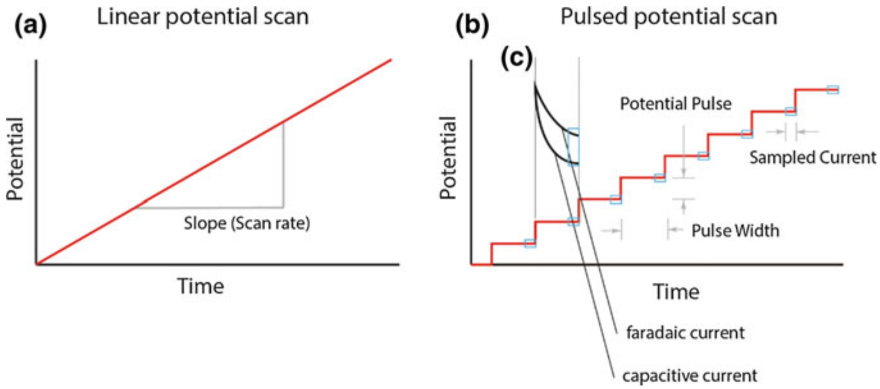

Fig. 2.5 Potential excitation waveforms for **a** linear sweep voltammetry and **b** pulse voltammetry **c** shows the behaviour of faradaic and capacitive currents as a function of time during a potential pulse

The current that flows in the cell is recorded as a function of time and thus as a function of the applied potential, resulting in a voltammogram. Among the parameters that need to be specified to record a voltammogram, the potential sweep rate is crucial. This parameter controls the slope of the potential variation as a function of time.

A typical response to a linear potential sweep is a peak-shaped voltammogram. The current starts to rise when the potential values match those of an electrode process. This creates a concentration gradient of electroactive species between the electrode surface and bulk solution, with the lack of electroactive species on the electrode surface making the current fall.

2.1.3.1 Cyclic Voltammetry

The potential can also be cycled multiple times between two values, e.g. first being increased linearly and then lowered at the same rate (Fig. 2.6).

Fig. 2.6 Cyclic voltammetry potential excitation signal

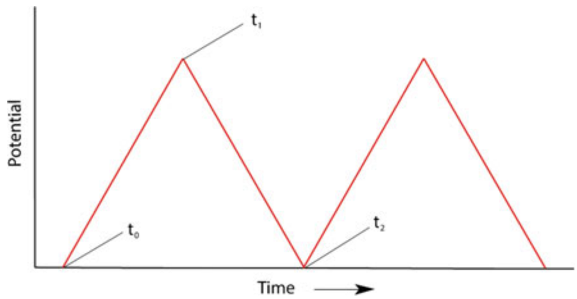

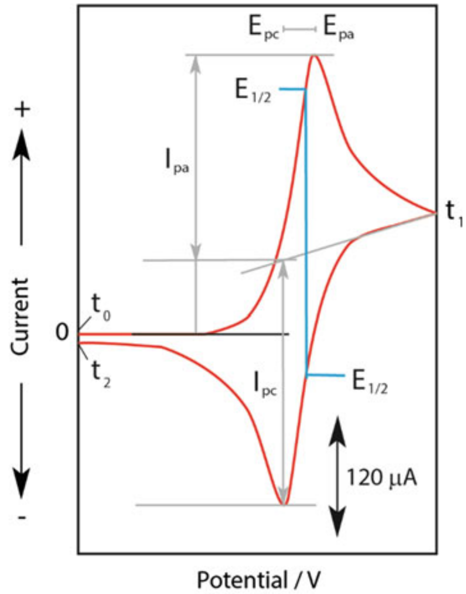

Fig. 2.7 A typical peak-shaped cyclic voltammogram. The parameters t_0, t_1, and t_2 are shown in Fig. 2.6

In cyclic voltammetry of reversible systems (i.e. ones with fast electrode kinetics relative to the potential sweep timescale), the product of initial oxidation or reduction can be regenerated by reversing the scan direction (Fig. 2.7). The following equation relates the peak current with other parameters of linear sweep voltammetry:

$$I_p = 2.69 \times 10^{-5} n^{\frac{3}{2}} A D^{\frac{1}{2}} C v^{\frac{1}{2}} \tag{2.10}$$

where I_p is the current peak in A, n is the number of electrons transferred in the electrode process, A is the electrode active area in cm^2, D is the diffusion coefficient of electroactive species in $cm^2\ s^{-1}$, C is the concentration of electroactive species in mol cm^{-3}, and v is the potential scan rate in $V\ s^{-1}$.

For reversible systems, (i) the ratio of oxidation and reduction current peak values (anodic and cathodic current peaks, I_{PA} and I_{PC}, respectively) is close to one and (ii) the separation between the cathodic and anodic potential peaks (E_{PC} and E_{PA}, respectively) is equal to 59.0/n mV, or equivalently:

$$E_{PC} = E_{\frac{1}{2}} - \frac{0.0285}{n} \tag{2.11}$$

$$E_{PA} = E_{\frac{1}{2}} + \frac{0.0285}{n} \tag{2.12}$$

For completely irreversible systems, only the oxidation or reduction process is detected, with no peak in the reversed sweep. Most of the redox couples are positioned between the completely reversible and irreversible systems (called *quasi*-reversible systems). In these cases, the reverse peak appears, but is smaller than the forward peak [5, 6, 10].

2.1.3.2 Hydrodynamic Voltammetry

Hydrodynamic electrodes can be employed as voltammetric sensors, subject to controlled convection imposed by solution or electrode movement. Convection enhances the mass transport of electroactive species to the electrode surface, so that the diffusion layer, with a concentration gradient present therein, is thinner than in the absence of convection. Consequently, the current response is enhanced. Hydrodynamic electrodes are important voltammetric sensors that operate under steady-state conditions. For analytical purposes, the sensors with highest sensitivity are those where a potential corresponding to the limiting current region is applied. If the rate of convective transport is constant, together with all the other control parameters, the current response of the electrode is also constant. These electrodes are usually operated under laminar flow conditions (in the absence of turbulence). The best-known hydrodynamic electrode is the rotating disc electrode. The limiting current for this electrode is given by:

$$I_{\mathrm{L}} = 1.554\,\pi rnFCD^{\frac{2}{3}}\upsilon^{-\frac{1}{6}}\omega^{\frac{1}{2}} \tag{2.12}$$

where r is the radius of the electrode in cm, F is the Faraday constant, C is the concentration of electroactive species in mol cm^{-3}, D is the diffusion coefficient in cm^2 s^{-1}, υ is the kinematic viscosity, and ω is the speed of rotation of the electrode in Hz [6, 10].

In some situations, electrodes are used in flow systems. There are many electrochemical flow cell detectors based on wall-jet or channel-tube electrodes. Generally, these cells are designed for chromatography, capillary electrophoresis, flow injection analysis, or batch injection analysis.

2.1.3.3 Microelectrode Voltammetry

Microelectrodes are electrodes with at least one dimension in the micrometre range. This minute dimension leads to low capacitive current contributions and the possibility of registering steady-state currents in a short time (Fig. 2.8). Microelectrodes have many advantages compared to conventional electrodes: (i) insertion of microelectrodes in places where other electrodes are too large; (ii) high

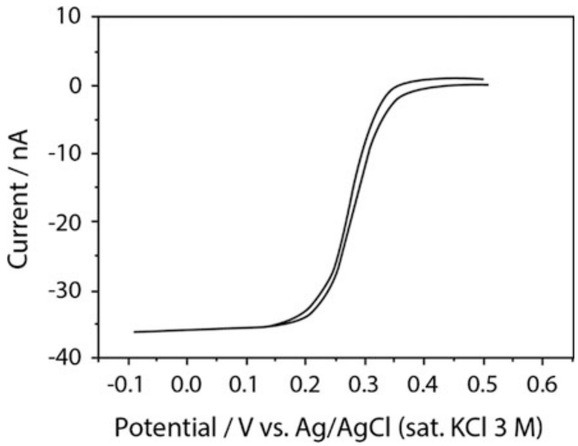

Fig. 2.8 A typical microelectrode cyclic voltammogram

signal/noise ratio; (iii) possibility of registering voltammograms in highly resistive media without the addition of an inert electrolyte; and (iv) relative insensitivity to forced convection of the solution. For a microdisc electrode, the steady-state current in the limiting current region is given by the following equation [10]:

$$I_{\mathrm{L}} = 4nFDCr \tag{2.13}$$

2.1.3.4 Pulsed Voltammetric Techniques

Pulse techniques are based on the current response to a sequence of potential steps in the forward and/or reverse directions. This response is a pulse of current that decreases with time as the electroactive species is consumed in the region near the electrode surface.

The registered current has a contribution from both faradaic and capacitive processes. The capacitive current decreases faster than the faradaic current. Thus, the current is usually sampled after the capacitive contribution becomes very low. Pulse widths are adjusted to achieve this condition (Fig. 2.5).

The most frequently used pulse techniques are differential pulse voltammetry and square wave voltammetry. Conceptually, the two techniques are very similar. The detection limits are of the order of 10^{-7} mol L^{-1} for differential pulse voltammetry and 10^{-8} mol L^{-1} for square wave voltammetry [5, 10].

2.1.3.5 Membrane and Modified Electrodes

There are many situations when controlling the potential is not sufficient to gain selectivity in voltammetric experiments. Response overlap can occur due to the proximity of electroactive species potentials or electrode kinetic processes. In some cases, the current response decreases with time due to blocking of the electrode surface by strongly adsorbed species. These problems can be circumvented by using modified electrodes as voltammetric sensors. Usually, the modification of electrodes brings selectivity by: (i) creation of physical barriers/membranes that block interfering species or (ii) deposition of material that reacts with the analyte more selectively or acts as a mediator for electron transfer.

Porous membranes can be used in voltammetric sensors, covering the electrode surface directly or having a thin layer of separating electrolyte. These membranes can act as size exclusion separators (blocking larger species like proteins) or as a gas-permeable membrane (as in the Clark oxygen electrode).

The use of enzymes immobilized on the electrode surface directly or within a membrane covering the electrode also allows to achieve high specificity. These biosensors combine electrochemical signal transduction with a biological sensing component.

In modified electrodes, changes are promoted in the surface layers of the electrode. Alternatively, a new layer at the electrode surface is formed to gain selectivity. The general intention is to enhance or facilitate some electrode processes while inhibiting other ones. There are many strategies for voltammetric sensor modification, including adsorption, chemical modification, electrodeposition, and surface treatment [11].

2.1.3.6 Other Techniques

Important information about the electroactive species, such as the number of transferred electrons and the diffusion coefficient, can be gained using techniques such as chronoamperometry (recording current as a function of time) and coulometry or chronocoulometry (recording charge as a function of time).

In AC voltammetry, a small amplitude sine wave is superimposed on a programmed potential variation. The perturbation of the system results in current responses that vary in amplitude and phase angle. The obtained voltammograms can provide information on the kinetics, and the response can be useful for analytical determinations. The in-phase and out-of-phase current components are related to faradaic currents and the separation of charging currents, respectively. Generally, this technique allows to achieve low detection limits, but processes with slow electrode kinetics result in the loss of sensitivity [5, 6, 10].

2.2 Colorimetric Sensors and Strategies for Extracting Colorimetric Information

In its early years, chemical analysis, either qualitative or quantitative, was performed using reagent-based colorimetric tests. After the rise of the instrumental methods of analysis, quantitative titration was practically abandoned. On the other hand, qualitative and/or semi-quantitative spot tests are still popular [12], with the use of pH colour-fixed indicators being a popular example.

The most typical instrumental way to obtain information on solution colour is to use a spectrophotometer or a photometer operating in the visible spectral range (400–800 nm), based on transmittance/absorbance measurement. Briefly, in absorption spectroscopy, the radiation intensity from a source of light at a specific wavelength is attenuated by passing through a coloured solution in a cuvette that is situated between the light source and a detector. The mathematical description of this process is known as the Beer–Lambert law (Eqs. 2.14 and 2.15):

$$T = \frac{I}{I_0} \tag{2.14}$$

$$A = -\log \frac{I}{I_0} \tag{2.15}$$

where T is the transmittance of the radiation passing through the solution, I_0 is the total intensity of the radiation source, I is the intensity of the radiation after passing through the solution, and A is the solution absorbance. The choice of wavelength (λ) to monitor coloured species is determined from the visible absorption spectra plot (A vs. λ), which may be performed sweeping the wavelengths in the visible spectral range. Often, the maximum absorption wavelength (λ_{max}) is used, mainly because it provides higher sensitivity. Absorption is proportional to the concentration and length of the cuvette optical path, as can be inferred from Eq. 2.16. Longer beam paths of the incident radiation increase the probability of the coloured species absorbing a part of this radiation:

$$A = \varepsilon bc \tag{2.16}$$

where ε is the molar absorption in cm^{-1} mol^{-1} L, b is the optical path in cm, and c is the concentration of the coloured species in mol L^{-1}. Figure 2.9 shows a simple scheme of the instrumentation used.

A classical application of spectrophotometric measurements is the indirect colorimetric quantification of glucose in biological fluids. This method is based on the reaction of glucose with glucose oxidase to produce hydrogen peroxide. The latter reacts with a chromogenic oxygen acceptor in the presence of peroxidase, producing a chromogenic species, which is spectrophotometrically monitored at 460 nm [8].

Even after the rise of portable spectrophotometers and the decrease of their price, the search for alternative ways of analytical colorimetric measurements continued.

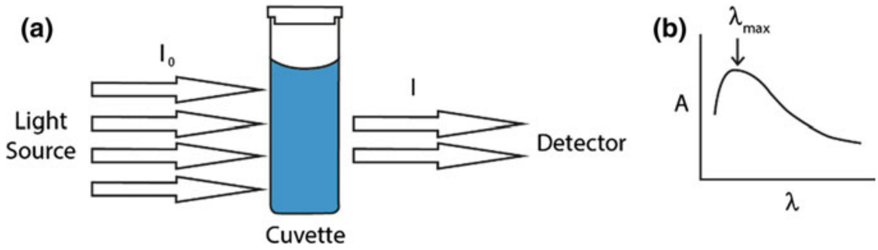

Fig. 2.9 **a** Scheme of the visible radiation absorption process. **b** Resultant absorbance (A) versus wavelength (λ) plot

Recently, various research groups have used desktop or portable scanners [14], digital cameras, webcams [15], cell phones, and smartphones [16] to collect analytical information based on colour measurement. In these methods, the reflection of the system was used, instead of the traditional way of measuring transmittance/absorbance. This is, therefore, an advantage, allowing the analysis of turbid samples [17].

Among the colour systems used, the most common way to process analytical data from digital images is based on the RGB colour model, which is used in computer screens and utilizes the primary colours of light. This is an additive model, and the name comes from the three primary colours: red (R), green (G), and blue (B), also called channels. In computers, each of these three channels is represented by an integer number from 0 to 255, and each combination represents a particular colour, making it possible to represent more than 16 million combinations (256^3 = 16,777,216). White colour, for example, is obtained when all three channels have values of 255, while black corresponds to all channels equal to zero. Some researchers use the H parameter (hue) of the HSV colour space [18, 19], which can be correlated with the RGB system, to monitor a specific coloured reaction. The extraction of the RGB code of a digital image can be performed by software [20, 21] or by a smartphone app. These apps may be home-made [22] or downloaded from popular virtual stores [23] of the operating system, such as iOS and Android. In addition, it is possible to convert the RGB colour model to other models, such as grayscale and CMYK (cyan, magenta, yellow, and black/key). The CMYK colour model, used for colour printing, is a subtractive system and uses secondary colours created by mixing two primary ones (RGB model). For example, mixing red and blue colours gives magenta [24]. An alternative way to record analytical colour information without the use of any sophisticated instrumentation was proposed by Cate et al. [25]. The authors explored the microfluidic properties of filter paper to propose a paper-based analytical device (μPAD), shaped as a strip and limited by a wax barrier, which was spotted with reagents giving a coloured reaction. A simple measurement of the reaction extent distance, using a ruler, was correlated with the concentration of the analyte [25]. The use of Google Glass to perform diagnostic colorimetric tests has also been proposed [26].

Various ways of treating the RGB data in a digital image are described in the literature. A widespread method is to find a channel (R, G, or B) that correlates linearly with the analyte concentration [26, 27, 28]. However, the use of grayscale and CMYK models has also been reported [16] in quantitative methods. Instead of using the classical above-mentioned method of glucose quantification, it was demonstrated that the information obtained from digital images can also be used for the same purpose. Researchers adopted the μPAD approach using a camera phone and a portable scanner as a detection system for the development of a colorimetric spot test to quantify glucose and protein content in synthetic urine [16]. Focusing on the glucose test, the method is similar to the classical one, i.e. the glucose is oxidized by glucose oxidase to gluconic acid, generating hydrogen peroxide. The peroxide is promptly reduced by iodide (catalysed by horseradish peroxidase) to give iodine, and the colour of the paper spot test region changes from colourless to brown. All reagents used in the assays were prespotted on the respective test zone of the paper, and the colour digital image, taken after exposing the μPAD to a synthetic urine sample, was converted to grayscale by software, with the mean intensity taken as an analytical signal [16].

Others approaches are based on the use of colour data from digital images coupled with widespread chemometrical tools [29], such as principal component analysis (PCA) [20, 22, 23, 30, 31], hierarchical cluster analysis (HCA) [22, 30, 32, 33], principal component regression (PCR) [21], partial least squares (PLS) [17, 29], soft independent modelling by class analogy (SIMCA) [35–38], linear discriminant analysis (LDA) [34–37], *k*-nearest neighbour (*k*-NN) [31], and artificial neural network (ANN) [18, 19]. These mathematical tools can replace the analysis performed by naked eye, avoiding major errors, especially when the method is based on spot tests. Illustrating the application of chemometrical tools and the use of colour images in analysis, Huang et al. [39] reported an array of colorimetric sensors, called an electronic nose (E-nose), based on a reversed-phase silica gel plate overprinted with specific dyes for the evaluation of fish freshness, as shown in Fig. 2.10.

Fig. 2.10 Profile of the colorimetric sensor array (E-nose) for the evaluation of fish freshness prior to being exposed to analytes. Reprinted from Huang et al. [39]. Copyright (2011), with the permission from Elsevier

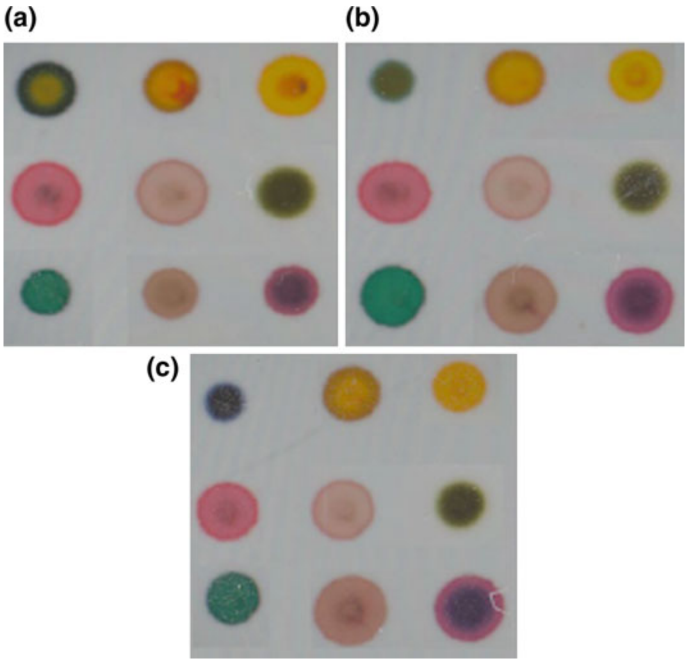

Fig. 2.11 Colour profiles of the E-nose after exposure to a fish sample at **a** day 1, **b** day 4, and **c** day 7. Reprinted from Huang et al. [39]. Copyright (2011), with the permission from Elsevier

The dyes were chosen with respect to the main volatile organic compounds (VOCs) released during the fish spoilage process. When these VOCs react with the dyes during the time of exposure, a change in the colour profile results, as shown in Fig. 2.11.

The sensor array was placed in a reaction chamber containing VOCs released by the fish sample, and images of the sensor were taken using a desktop scanner. The images were recorded before and after exposure to VOCs at different times. Next, a difference map of the images was obtained by subtracting the images after exposure to VOCs from those taken before the exposure and converting the result into RGB values. These values were used as input data to perform principal component analysis. The authors observed that the first-day data were dispersed on a smaller area when compared to that for the second through fifth days. This observation is probably due to the fact that on the first-day, the fish was still fresh, while between the second and fifth days, the fish released new VOCs owing to the deterioration process. It was also noted that the data group for the sixth and seventh days of the storage is easily separable from other data, once the fish begins to release a large amount of biogenic amines. Thus, the authors used the data obtained by PCA to build a model with a neural network approach, obtaining an accuracy about 87.5 % [39]. Although the authors used a desktop scanner to collect RGB data, it is easily possible to use a smartphone, which is a ubiquitous gadget. The use of a smartphone with an app that could readily perform a scan of the colorimetric sensor array placed in the package of the product stored in a supermarket, for example, was proposed by Bueno et al. [22]. This can help the consumer avoid buying a spoiled product.

In contrast, the use of the above-mentioned devices to take digital images in order to perform analytical inferences about the subject matter is not so simple and shows some drawbacks. Different devices can produce different images, i.e. different RGB values for the same region, which is not always easy to spot with the naked eye [40, 41]. The resolution of the device, the technology used to build it, the shooting distance, and the imaging angle are some examples of factors that may contribute to providing different RGB values for the same target. Besides, luminosity control at the moment a digital image is taken is of paramount importance and is another factor of concern that influences RGB values [28, 30, 42]. However, researchers have designed strategies to circumvent this problem. Usually, a black chamber with controlled luminosity and a fixed position of device components is used [22, 28, 30, 43] to capture the images before (blank) and after exposure to the analyte, and thus, the images are subtracted directly (difference map). Approaches that try to compensate for the influence of the illumination conditions, cell phone/smartphone model, distance, and angle to the substrate, without the use of an extra accessory, have been proposed [33, 44, 45].

References

1. Mendham J, Denney RC, Barnes JD, Thomas MJK (1979) Vogel's quantitative chemical analysis, 5th edn. Wiley, New York
2. Pungor E (1965) Oscillometry and conductometry, 1st edn. Pergamon Press, Budapest
3. Fracassi da Silva JA, do Lago CL (1998) An oscillometric detector for capillary electrophoresis. Anal Chem 70:4339–4343. doi:10.1021/ac980185g
4. Cordeiro JR, Martinez MIV, Li RWC et al (2012) Identification of four wood species by an electronic nose and by LIBS. Int J Electrochem 2012:1–5. doi:10.1155/2012/563939
5. Brett CMA, Brett AMO (1993) Electrochemistry: principles, methods, and applications, 1st edn. Oxford University Press, New York
6. Wang J (2006) Analytical electrochemistry, 3rd edn. WILEY-VCH, New Jersey
7. Amemiya S (2007) Potentiometric Ion-Selective Electrodes. In: Zoski CG (ed) Handbook of electrochemitry, 1st edn. Elsevier Science, Amsterdam, p 935
8. Jimenez-Jorquera C, Orozco J, Baldi A (2010) ISFET based microsensors for environmental monitoring. Sensors (Basel) 10:61–83. doi:10.3390/s100100061
9. Brett CMA, BRETT AMO (1998) Electroanalysis, 1st edn. Oxford University Press, New York
10. Bard AJ, Faulkner LR (1990) Electrochemical methods: Fundamentals and applications. Wiley, New York

11. Edwards GA, Bergren AJ, Porter MD (2007) Chemically Modified Electrodes. In: Zoski CG (ed) Handbook of electrochemistry, 1st edn. Elsevier Science, Amsterdam, p 935
12. Byrne L, Barker J, Pennarun-Thomas G et al (2000) Digital imaging as a detector for generic analytical measurements. TrAC Trends Anal Chem. 19:517–522. doi:10.1016/S0165-9936(00)00019-4
13. Bergmeyer H-U, Bernt E (1965) Determination with glucose oxidase and peroxidase. In: Bergmeyer H-U (ed) Methods of enzymatic analysis. Elsevier, London, pp 123–130
14. Carey JR, Suslick KS, Hulkower KI et al (2011) Rapid identification of bacteria with a disposable colorimetric sensing array. J Am Chem Soc 133:7571–7576. doi:10.1021/ja201634d
15. Gaiao EN, Martins VL, Lyra W da S, et al (2006) Digital image-based titrations. Anal Chim Acta 570:283–290. doi:10.1016/j.aca.2006.04.048
16. Martinez AW, Phillips ST, Carrilho E et al (2008) Simple telemedicine for developing regions: camera phones and paper-based microfluidic devices for real-time, off-site diagnosis. Anal Chem 80:3699–3707. doi:10.1021/ac800112r.Simple
17. Abbaspour A, TalebanpourBayat E, Mirahmadi E (2012) A reliable and budget-friendly, solution-based analysis of multiple analytes of boiler water based on reflection scanometry. Anal Methods 4:1968. doi:10.1039/c2ay05799a
18. Ariza-Avidad M, Salinas-Castillo A, Cuéllar MP et al (2014) Printed disposable colorimetric array for metal ion discrimination. Anal Chem 86:8634–8641. doi:10.1021/ac501670f
19. Ariza-Avidad M, Cuellar MP, Salinas-Castillo A et al (2013) Feasibility of the use of disposable optical tongue based on neural networks for heavy metal identification and determination. Anal Chim Acta 783:56–64. doi:10.1016/j.aca.2013.04.035
20. San Park T, Baynes C, Cho S-I, Yoon J-Y (2014) Paper microfluidics for red wine tasting. RSC Adv 4:24356–24362. doi:10.1039/C4RA01471E
21. Firdaus ML, Alwi W, Trinoveldi F et al (2014) Determination of chromium and iron using digital image-based colorimetry. Procedia Environ Sci 20:298–304. doi:10.1016/j.proenv.2014.03.037
22. Bueno L, Meloni GN, Reddy SM, Paixão TRLC (2015) Use of plastic-based analytical device, smartphone and chemometric tools to discriminate amines. RSC Adv 5:20148–20154. doi:10.1039/C5RA01822F
23. Vallejos S, Muñoz A, Ibeas S et al (2013) Solid sensory polymer substrates for the quantification of iron in blood, wine and water by a scalable RGB technique. J Mater Chem A 1:15435. doi:10.1039/c3ta12703f
24. Galer M, Horvat L (2005) Digital imaging, 3rd edn. Elsevier, Oxford
25. Cate DM, Dungchai W, Cunningham JC et al (2013) Simple, distance-based measurement for paper analytical devices. Lab Chip 13:2397. doi:10.1039/c3lc50072a
26. Feng S, Caire R, Cortazar B, et al (2014) Terms of use immunochromatographic diagnostic test analysis using Google Glass. ACS Nano 3069–3079
27. Abbaspour A, Mehrgardi MA, Noori A et al (2006) Speciation of iron(II), iron(III) and full-range pH monitoring using paptode: A simple colorimetric method as an appropriate alternative for optodes. Sens Actuators B Chem 113:857–865. doi:10.1016/j.snb.2005.03.119
28. Benedetti LPDS, dos Santos VB, Silva TA et al (2015) A digital image-based method employing a spot-test for quantification of ethanol in drinks. Anal Methods 7:4138–4144. doi:10.1039/C5AY00529A
29. Diehl KL, Anslyn EV (2013) Array sensing using optical methods for detection of chemical and biological hazards. Chem Soc Rev 42:8596. doi:10.1039/c3cs60136f
30. Salles MO, Meloni GN, de Araujo WR, Paixão TRLC (2014) Explosive colorimetric discrimination using a smartphone, paper device and chemometrical approach. Anal Methods 6:2047–2052. doi:10.1039/C3AY41727A
31. Bueno L, Cottell A, Reddy SM, Paixão TRLC (2015) Coupling dye-integrated polymeric membranes with smartphone detection to classify bacteria. RSC Adv 5:97962–97965. doi:10.1039/C5RA19874G

32. Suslick KS, Rakow NA, Sen A (2004) Colorimetric sensor arrays for molecular recognition. Tetrahedron 60:11133–11138. doi:10.1016/j.tet.2004.09.007
33. Jia M-Y, Wu Q, Li H et al (2015) The calibration of cellphone camera-based colorimetric sensor array and its application in the determination of glucose in urine. Biosens Bioelectron 74:1029–1037. doi:10.1016/j.bios.2015.07.072
34. Garrido-Novell C, Pérez-Marin D, Amigo JM et al (2012) Grading and color evolution of apples using RGB and hyperspectral imaging vision cameras. J. Food Eng 113:281–288. doi:10.1016/j.jfoodeng.2012.05.038
35. Costa GB, Fernandes DDS, Almeida VE et al (2015) Digital image-based classification of biodiesel. Talanta 139:50–55. doi:10.1016/j.talanta.2015.02.043
36. Diniz PHGD, Dantas HV, Melo KDT et al (2012) Using a simple digital camera and SPA-LDA modeling to screen teas. Anal Methods 4:2648. doi:10.1039/c2ay25481f
37. Almeida VE, da Costa GB, de Sousa Fernandes DD et al (2014) Using color histograms and SPA-LDA to classify bacteria. Anal Bioanal Chem. 406:5989–5995. doi:10.1007/s00216-014-8015-1
38. Pedrosa VA, Caetano J, Machado SAS, Bertotti M (2008) Determination of parathion and carbaryl pesticides in water and food samples using a self assembled monolayer/acetylcholinesterase electrochemical biosensor. Sensors 8:4600–4610. doi:10.3390/s8084600
39. Huang X, Xin J, Zhao J (2011) A novel technique for rapid evaluation of fish freshness using colorimetric sensor array. J. Food Eng. 105:632–637. doi:10.1016/j.jfoodeng.2011.03.034
40. Dorsey J, Rushmeier H, Sillion F (2008) Digital modeling of material appearance, 1st edn. Elsevier, London
41. Lasarte M De, Vilaseca M, Pujol J, et al (2005) Influence of technology, color architecture and bit-depth of optoelectronic imaging sensors used as color measurement instruments. In: Congress of the International Colour Association. pp 1203–1206
42. García A, Erenas MM, Marinetto ED et al (2011) Mobile phone platform as portable chemical analyzer. Sensors Actuators B Chem 156:350–359. doi:10.1016/j.snb.2011.04.045
43. Steiner M-S, Meier RJ, Duerkop A, Wolfbeis OS (2010) Chromogenic sensing of biogenic amines using a chameleon probe and the red—green—blue readout of digital camera images. Anal Chem 82:8402–8405. doi:10.1021/ac102029j
44. Hong J Il, Chang B-Y (2014) Development of the smartphone-based colorimetry for multi-analyte sensing arrays. Lab Chip 14:1725–1732. doi:10.1039/c3lc51451j
45. Gupta R, Reifenberger RG, Kulkarni GU (2014) Cellphone camera imaging of a periodically patterned chip as a potential method for point-of-care diagnostics. ACS Appl Mater Interfaces 6:3923–3929. doi:10.1021/am4050426

http://www.springer.com/978-3-319-47833-3

Materials for Chemical Sensing
Cesar da Paixão, T.R.L.; Reddy, S.M. (Eds.)
2017, IX, 268 p. 126 illus., 98 illus. in color., Hardcover
ISBN: 978-3-319-47833-3